
Geoarchaeology of the Nehalem Spit: Redistribution of Beeswax Galleon Wreck Debris by Cascadia Earthquake and Tsunami (~A.D. 1700), Oregon, USA

Curt D. Peterson,^{1,*} Scott S. Williams,²
Kenneth M. Cruikshank,¹ and John R. Dubè³

¹Portland State University, Portland, Oregon 97207

²Washington State Department of Transportation, Olympia, Washington 98501

³P.O. Box 212, Manzanita, Oregon 97130

A coincidence of the Beeswax galleon shipwreck (ca. A.D. 1650–1700) and the last Cascadia earthquake tsunami and coastal subsidence at ~A.D. 1700 redistributed and buried wreck artifacts on the Nehalem Bay spit, Oregon, USA. Ground-penetrating radar profiles (~7 km total distance), sand auger probes, trenches, cutbank exposures (29 in number), and surface cobble counts (49 sites) were collected from the Nehalem spit (~5 km² area). The field data demonstrate (1) the latest prehistoric integrity of the spit, (2) tsunami spit overtopping, and (3) coseismic beach retreat since the A.D. 1700 great earthquake in the Cascadia subduction zone. Wreck debris was (1) initially scattered along the spit ocean beaches, (2) washed over the spit by nearfield tsunami (6–8 m elevation), and (3) remobilized in beach strandlines by catastrophic beach retreat. Historic recovery of the spit (150 m beach progradation) and modern foredune accretion (>5 m depth) have buried both the retreat scarp strandlines and associated wreck artifacts. The recent onshore sand transport might re-expose heavy ship remains in the offshore area if the wreck grounded in shallow water (<20 m water depth of closure).

© 2011 Wiley Periodicals, Inc.

INTRODUCTION

In this paper we propose a mechanism for the dispersal and burial of Beeswax wreck debris on the Nehalem spit at about A.D. 1700 (Figure 1). Recovered debris from this wreck is reported to include substantial quantities of beeswax blocks and candles, teak ship's timbers, and Chinese porcelains (Hult, 1968; Marshall, 1984; Woodward, 1986a, 1986b). The extensive deposits of beeswax blocks and candles found widely spread around Nehalem Spit and Bay throughout the 19th century lent their name to the vessel, which wrecked prior to European exploration and settlement of this part of the coast (Marshall, 1984; Williams, 2008).

Large teak timbers were reportedly recovered during the mid to late 19th and early 20th centuries from the interior of the northern end of the Nehalem sand spit

*Corresponding author; E-mail: petersonc@pdx.edu.

PETERSON ET AL.

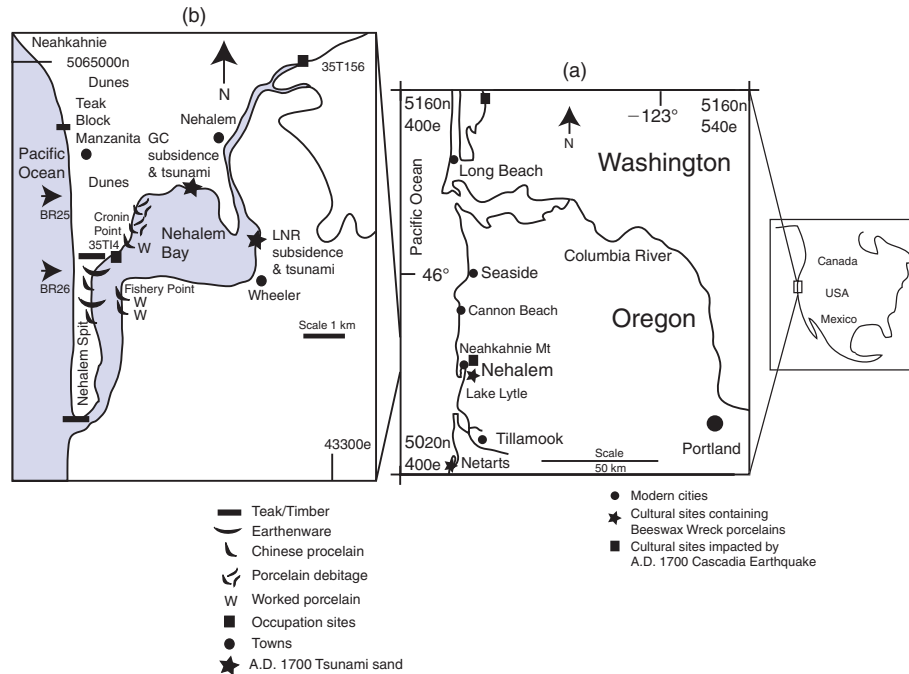


Figure 1. Location of Nehalem Bay in northern Oregon (a), including locations of Beeswax wreck artifacts reported from prehistoric sites (solid stars), and Native American occupation sites reported to have been impacted by the last great Cascadia earthquake at A.D. 1700 (solid squares). Distribution of Beeswax wreck artifacts and other archaeological sites in Nehalem Bay (b). Teak wood timber (solid bar), teak wood blocks (solid rectangle), worked Chinese porcelain sherds (W), and unworked porcelain and earthenware sherds are shown, as reported (Woodward, 1990; Giesecke, 2007). The Cronin Point midden sites are identified as 35T14. Coseismic subsidence records are reported from the lower Nehalem River (LNR) (Grant, 1994). The Manzanita dune field ramps up the southern flank of the Neahkahnie headland, at the northern end of the Tillamook littoral cell (Cooper, 1958; Peterson et al., 2010). Estimates of potential beach retreat (arrows) have been predicted for two sites BR25 and BR26 (Doyle, 1996). Reference coordinates are in UTM northing (n) and easting (e) in meters.

(Figure 1) (Marshall, 1984; Giesecke, 2007). The beeswax and porcelains were more widely distributed by currents and/or by Native American transport and trading (Beals & Steele, 1981; Scheans & Stenger, 1990). The presence of the heavy teak timber in the spit interior has led to speculation that channels dissected the spit, permitting the wreck debris to float across the sand barrier. However, the main hull and heavy cargo, such as cannons and anchors, of the wrecked vessel have never been found. The Beeswax wreck was likely an important event in early contact between Oregon coast Native Americans and Europeans (Erlandson, Losey, & Peterson, 2001).

Teak wood and beeswax were found along the Nehalem spit ocean beach and the Nehalem bay flats through the 1800s (Hult, 1968; Marshall, 1984; Williams, 2008; Figure 1). The beeswax artifacts range from candles to large blocks weighing more

GEOARCHAEOLOGY OF THE NEHALEM SPIT

than 80 kg (Giesecke, 2007). Beeswax samples have been radiocarbon dated, with samples dated in the 1960s and 1980s yielding date ranges of A.D. 1485–1800, with the most likely overlaps being from 1600 to 1700 (Erlandson, Losey, & Peterson, 2001; Williams, 2007). A sample dated by high-precision accelerator mass spectrometry (AMS) dating in 2008 yielded a date range of 1660–1800 (Beta 249345). Many of the beeswax blocks are reported to have the initials “IHS” or symbols carved into them, typical of Spanish shipping marks (Marshall, 1984; Giesecke, 2007).

Efforts to identify the wrecked ship have recently shifted to the use of the wreck’s porcelain sherds. The sherds date the wreck to the Spanish galleon trade from the Philippines to Mexico at about A.D. 1650–1700 (Lally, 2008). Using visual attributes, Lally (2008) derived a mean ceramic date of A.D. 1686. This ceramic date is based on 1189 sherds collected over a period (15 years) from the Nehalem area. Two possible galleon wrecks, as yet unaccounted for, include the *Santo Christo de Burgos* lost in A.D. 1693 and the *San Francisco Xavier* lost in A.D. 1705 (Levesque, 2002; Lally, 2008). The Oregon coast is well north of the normal Manila galleon trade routes (Schurz, 1939), leading to much speculation about the circumstances of the wreck in the Nehalem area (Giesecke, 2007; Marshall, 1984; Williams, 2007).

Some of the Chinese porcelain was flaked into tools by Native Americans, as shown by scattered debitage, finished points, and scrapers in Nehalem Bay (Figure 1). Other unworked porcelains and larger earthenware fragments have been found on the bay shoreline of the Nehalem spit (Figure 2). The earthenware fragments, thought to be storage jar fragments, are not suitable for tool making, so they were unlikely to have been traded or manually transported by the native populations. The recent, but rare, appearances of these earthenware fragments suggest that they are currently being released from bayside cutbanks of the Nehalem sand spit.

In this paper we review the geomorphic conditions and littoral processes that could account for the apparent dispersal of the Beeswax wreck debris across the Nehalem spit. The results presented here also address the episodic remobilization and exposure of wreck debris that are reported from the Nehalem beaches and bay spit shorelines. Coincidences between the archaeologically determined wreck age (A.D. 1680–1700) and the last Cascadia great earthquake (Mw 9) and tsunami at A.D. 1700 (Satake et al., 1996) are proposed to account for the across-spit dispersal of wreck debris. The disappearance of beach wreck debris by the early 20th century is related to historic beach recovery, following the earthquake-induced coseismic beach retreat (Peterson, Doyle, & Barnett, 2000).

STUDY AREA

The Nehalem spit is 5–6 km in length and ranges from 0.5 to 1.0 km in width (Figure 1). It is fronted by a large foredune of 10–15 m elevation (NAVD88). [The NAVD88 0 m datum is about 1 m below mean tidal level (MTL) in the study area.] The foredune vertically accreted to its present height since the middle 1900s due to the introduction of European dune grass. The spit narrows in its middle section, located 1–3 km south Cronin Point (Figures 1, 3). The narrow middle section of the spit is located adjacent to a right-angle bend of the Nehalem channel, opposite to

PETERSON ET AL.

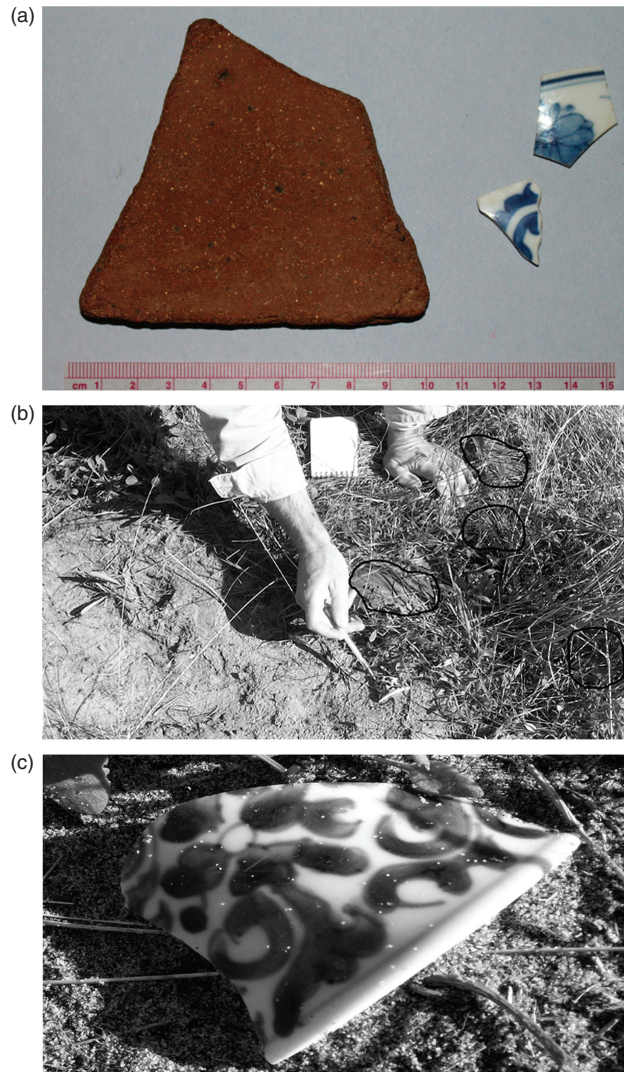


Figure 2. (a) Beeswax wreck ceramics from the Nehalem spit bay shoreline. Large earthenware fragment (10 cm size) and smaller porcelain fragments (1–2 cm size) are unworked. The porcelain fragments have not been rounded by wind or water abrasion, suggesting recent release from eroding cutbank sites. (b) Recently discovered Chinese porcelain from the spit interior (site CP#1), showing 6-cm-wide sherd, at end of hand held pen, in sand trail, and associated half-buried cobbles (dark line circles) in grass. (c) Enlargement of Chinese porcelain sherd showing blue-on-white floral scroll motif (photo by Gary McDaniel).

GEOARCHAEOLOGY OF THE NEHALEM SPIT

Fishery Point on the mainland (Figure 1). A deflation plain behind the foredune decreases in height from the spit interior (~5 m elevation) to cutbanks (~2 m elevation) along the bay shoreline.

The Nehalem spit developed at the northern end of the Tillamook littoral cell (Figure 1). Littoral drift reverses seasonally in the northern Oregon coast (Komar, 1992), but in the Nehalem area it is dominated by winter waves approaching shore from the southwest. A long-term net littoral transport to the north in the Nehalem littoral cell is demonstrated by the large build-up of sand in the Manzanita dune field on the southern slope of the Neahkahnie headland (Cooper, 1958; Peterson et al., 2009). Driftwood accumulates on the ocean beaches from the spit north to the Neahkahnie headland, located near the town of Manzanita. Some drift logs have been observed floating northward around the Neahkahnie headland during major winter storms.

Evidence for Cascadia Earthquakes in Nehalem Bay

Four abrupt subsidence events are recorded by buried peaty horizons in the Nehalem Bay wetlands (Table I), as reported by Grant (1994) at a lower Nehalem River site (LNR) and near a prehistoric archaeological site (35T156; Figure 1) (Minor & Grant, 1996). The dated subsidence events are correlated to the last four ruptures of the central Cascadia mega-thrust fault. The Cascadia subduction zone extends from British Columbia, Canada, to northernmost California, possibly producing Mw 9 earthquakes (Heaton & Kanamori, 1984). The last four ruptures in northern Oregon and southern Washington are regionally dated at 0.3 ka, 1.1 ka, 1.3 ka, and 1.7 ka (Darienzo, Peterson, & Clough, 1994; Darienzo & Peterson, 1995; Atwater et al., 2004). The Cascadia ruptures are associated with nearfield tsunami that are recorded by sand sheets in back-barrier wetlands (Cannon Beach) and back-barrier ponds (Crescent and Lytle barrage ponds) (Figure 1). The last Cascadia rupture could correlate to a historic farfield tsunami runup in Japan, dated to the year A.D. 1700, as reported by Satake et al. (1996).

Catastrophic Beach Retreat

The coseismic subsidence events in the northern Oregon Coast range from 0.5 to 1.5 m (Barnett, 1997), with the last event at A.D. 1700 representing about 1.5 m of subsidence in the Nehalem Bay area, Oregon (Grant, 1994). The coseismic subsidence submerged tidal marshes for decades to centuries (Barnett, 1997), and caused widespread catastrophic beach erosion (Doyle, 1996). The catastrophic beach erosion events are identified by retreat scarps (5–15 m in height), which are preserved in episodically prograded beach profiles (Meyers et al., 1996). The subsurface scarps are imaged by ground-penetrating radar (GPR) in large barrier beaches and beach plains located in Long Beach, Washington, and north of Seaside, Oregon, located on either side of the Columbia River mouth (Figure 1) (Woxell, 1998; Peterson et al., 2010).

PETERSON ET AL.

Table I. Radiocarbon dates of reported coseismic subsidence and associated tsunami or beach retreat events for Nehalem Bay (a), Crescent and Lytle Lakes (b), Cannon Beach (c), and Clatsop (d).

Impact/Age	Event 1 A.D. 1700	Event 2 ~1.1 ka	Event 3 ~1.3 ka	Event 4 ~1.7 ka
(a)				
Subsidence	1.5 m	0.5–1.0 m	0.5–1.0 m	1.5 m
Sample dates	$N = 12$	$N = 9$	$N = 2$	$N = 6$
Mean age yr B.P.	230 ± 18	846 ± 22	1395 ± 57	1752 ± 25
Calibrated yr B.P.	0–304	724–890	1260–1400	1608–1725
(b)				
Tsunami runup	Small	Medium	Large	
Mean age cal. B.P.	265	1145	1350	
(c)				
Subsidence	Large	Medium	Small	Large
Tsunami runup	~7 m	>8 m	>>8 m	
Age cal. B.P. 2σ	0–510	930–1280	1276–1411	
(d)				
Subsidence	1.5–2.0 m	1.0–1.5 m	0.5–1.0 m	1.5–2.0 m
Retreat Scarp	Large	Medium	Small	Large
Mean Age	0.3 ka	1.1 ka	1.3 ka	1.7 ka

Note: Regional Cascadia rupture ages (Events 1–4) from Atwater et al. (2004). Nehalem data from Grant (1994); Minor and Grant (1996). Crescent and Lytle Lakes data from Schlichting (2000) and Schlichting and Peterson (2006). Cannon Beach data from Peterson et al. (2008). Clatsop data from Peterson et al. (2010).

Potential beach retreat of about 100 m is predicted for two sites (BR25 and BR26) in the Nehalem spit area, following potential coseismic subsidence of 1.25 m (Figure 1) (Doyle, 1996). The beach retreat estimates are based on a modified Brunn Rule (Komar et al., 1991) and on modern across-shore profiles. Postseismic rebound and interseismic uplift should eventually return the displaced beach sand back to the shoreline. Assuming no net gain or loss of beach sand from the littoral cell, the interseismic beach recovery should accrete the shoreline back to pre-earthquake positions.

Tsunami Deposit Confirmation in Nehalem Bay

Tsunami sand sheets were not formally identified by Grant (1994) in the lower Nehalem River (LNR), but a 10-cm-thick layer of sand and silt was observed to directly overlie the uppermost buried wetland soil. To confirm the presence of A.D. 1700 tsunami deposits in Nehalem Bay, several cores (sites GC1–3) were taken at the northernmost margin of the lower Nehalem Bay (Figure 4). Only the shallowest buried wetland (~A.D. 1700) was targeted for paleotsunami deposition in this limited confirmation study of tsunami inundation in Nehalem Bay.

The criteria used to verify tsunami deposition in northern Oregon estuaries include (1) anomalous sand layer(s) directly overlying an abruptly buried marsh surface,

GEOARCHAEOLOGY OF THE NEHALEM SPIT



Figure 3. Middle portion of Nehalem bay spit. Photo taken from the Neahkahnie headland (view toward the southeast).

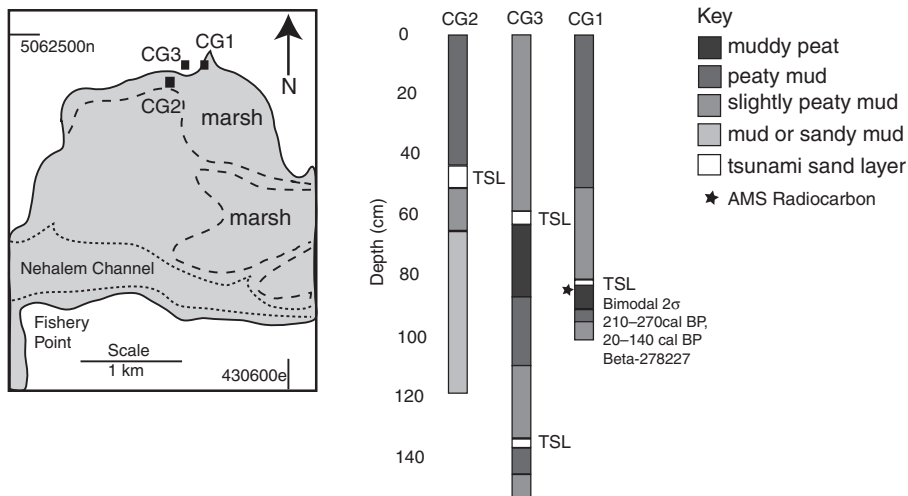


Figure 4. Map of core sites CG1-3 (above) and core logs (below) obtained to test for the presence of a tsunami sand sheet above the youngest (A.D. 1700) buried soil in the northernmost shoreline of Nehalem Bay.

(2) presence of well-rounded beach sand grains in the anomalous sand layer, (3) separation distance (~100 m) between anomalous sand layer sites and major channels or exposed sand flats, (4) fining-up sand to silt sequence with overlying organic debris cap, (5) continuity of anomalous sand sheet deposition between adjacent core sites, and (6) local landward thinning of the anomalous sand sheet (Peterson & Darienzo, 1997; Peterson et al., 2008). All of the criteria were met in the core sites (CG1–3) at the north end of Nehalem Bay (Figure 4).

PETERSON ET AL.

The GC paleotsunami locality is located about 2.0 km in distance from the main Nehalem channel, and about 3.5 km from the middle section of the Nehalem spit. The first buried wetland soil (muddy peat) is overlain by a thin sand layer (3–6 cm in thickness) that fines upward to a silt and/or organic debris cap. The buried soil in GC1 at 84 cm depth yields 2-sigma dates of 210–270 cal. B.P. and 20–140 cal. B.P. (Beta #278227). The bimodal calibration curve results obtained for this shallowest buried soil are not unexpected due to high radiocarbon production at about A.D. 1700, and to potential descending roots from the post-rebound marsh. Our objective here is to discriminate between the A.D. 1700 tsunami and older events at 800 to 1000 yr B.P. (Peterson et al., 2008). The reported age(s) for the buried soil in GC1 at 84 cm depth reflects paleotsunami inundation and coseismic subsidence from the last Cascadia rupture at A.D. 1700. The sand layer represents tsunami inundation(s) well landward of the Nehalem Bay spit. Inundation from the A.D. 1700 tsunami might have reached a subsidence-impacted archaeology site 35T156 (Figure 1) at a distance of 10 km upriver from the Nehalem spit (Minor & Grant, 1996).

Early Historic Geomorphology of Nehalem Bay

Several features of the Nehalem spit suggest recent instability, including its relatively thin aspect, the acute southward deflection of the Nehalem River channel, and the low heights (3–5 m elevation) of the spit interior. However, the early survey maps of the Nehalem coast (U.S. Coast Survey, 1875) show the spit extending south of the present tidal inlet (Figure 5). The presence of Beeswax wreck timber in the spit interior could argue for (1) a tidal inlet channel breach of the spit, or (2) a more landward position of the spit shoreline at the time of the shipwreck. Some spit interior sites that are reported to have yielded Beeswax wreck debris range from 6 to 8 m elevation (Figure 1). These elevations exceed the expected maximum combined reach of tides (~3 m elevation) and sustained storm surge (1.5 m) on the Oregon coast (Pitcock et al., 1982). Nevertheless, the first geoarchaeological investigation in this study focused on the possibilities of (1) tidal inlet breaching of the middle section of the spit, and (2) changing beach shoreline positions in the Nehalem spit.

METHODS

Ground-Penetrating Radar Profiling

Ground-penetrating radar (GPR) was used to profile the Nehalem spit for evidence of tidal inlet breaches and changes in shoreline position. A PulseEkko 100A system, with 50 MHz antennae and 900 V transmitter, was used for profiling the spit at 0.5 or 1.0 m step spacing. Digital stacking of 16 or 32 pulses per trace was used to increase signal-to-noise ratio. Penetration generally reached 10–20 m depth, based on a velocity of 0.08 m ns^{-1} in the saturated barrier sand (Jol, Smith, & Meyers, 1996). Profiles were collected along the spit (north to south) and across the spit (east to west) (Figure 6). Elevation control for the along-spit profiles is based on interpolations

GEOARCHAEOLOGY OF THE NEHALEM SPIT

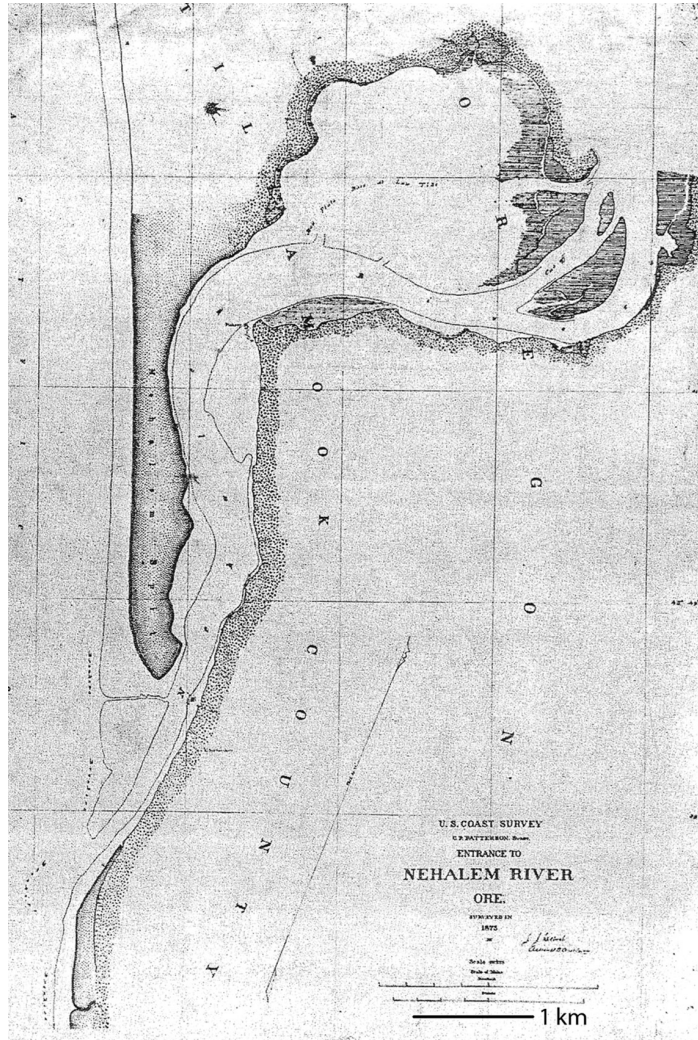


Figure 5. Historic (1875) Nehalem spit shoreline map. Map from U.S. Coast Survey (1875). Grid lines are aligned north-south (vertical) and east-west (horizontal).

between 3 m contours from U.S. Geological Survey topographic maps (± 1.5 m NAVD88) at endpoints georeferenced by GPS wass-12 channel (± 5 m EPE). Elevation control for the across-spit profiles is based on total station surveying to registered bench marks (± 0.1 m elevation NAVD88). All GPR profiles are processed with adjusted gain control (AGC) to enhance reflections at depth (Jol & Bristow, 2003).

PETERSON ET AL.

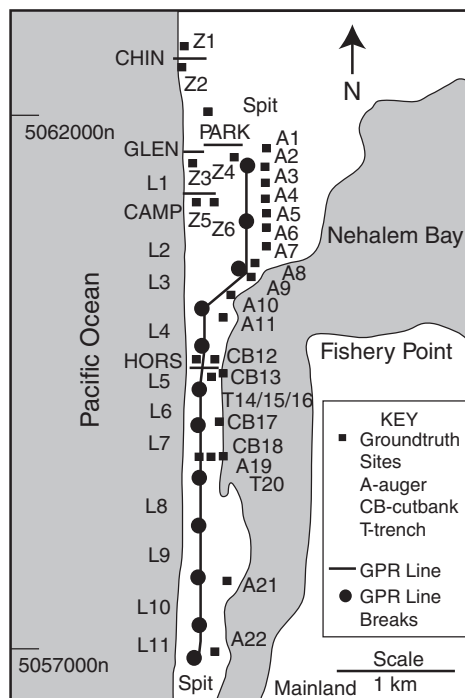


Figure 6. Ground-penetrating radar (GPR) profiles (bold lines) and shallow groundtruthing sites (solid squares) including auger probes (A and Z) trenches (T), and cutbanks (CB) in the Nehalem spit. GPR lines are numbered (L1–L11) for north-to-south profiles, and are named (four-letter street abbreviation) for east-to-west profiles. UTM coordinates and stratigraphic data for groundtruth sites are provided in Table II. Map reference coordinates are in UTM northing (n) in meters.

Groundtruthing of the GPR profiles was completed by hand probing with sand auger (7.5 cm diameter), shovel trench (1–2 m length), and examination of bay shoreline cutbanks (Figure 6).

Following observations of surface cobbles in dune deflation hollows from the spit interior, a systematic search was conducted for large-clast distribution along the full length of the spit. A total of 104 grids (100 × 100 m in size) were searched for the presence of grouped pebbles, cobbles, and boulders exposed at the surface. About one-half of the grids (49 in number) contained exposures of grouped large clasts, usually located in deflation hollows, trails, or pond margins in the spit (Figure 7). The first site found in each grid was then analyzed for clast abundance and size distribution in measured plot areas (0.5 m², 1.0 m², 10 m² surface areas). Clast intermediate diameters (Di) were measured to the nearest 0.1 cm. Site positions were georeferenced using GPS or Total Station-OPUS surveying.

GEOARCHAEOLOGY OF THE NEHALEM SPIT

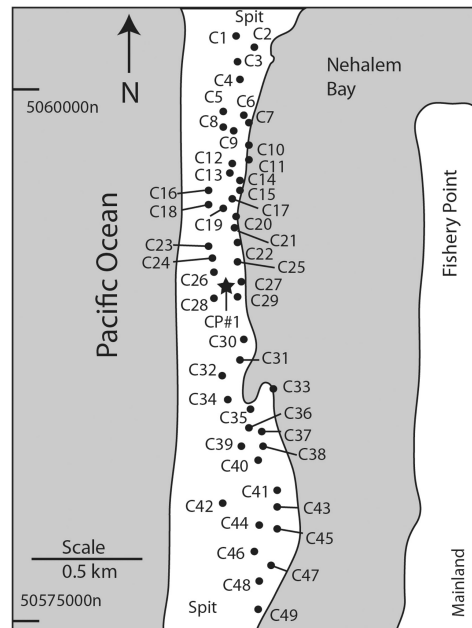


Figure 7. Surface cobble sites (black circles) measured for frequency and size distributions of exposed large clasts (pebble, cobble, and boulder) in the Nehalem sand spit. Recently discovered Chinese porcelain sherd is denoted by the site CP#1 (black star) in the exposed cobble sheet from the interior of the central spit. Cobble and Chinese porcelain sherd site UTM coordinates and clast data are presented in Table III. Map reference coordinates are in UTM northing (n) in meters.

RESULTS

The earliest historic stability of the Nehalem spit was tested for tidal inlet breaches by continuous GPR profiling from north to south along a packed sand–gravel access road (Figure 6). GPR penetration reached 10–15 m depth, with abrupt signal loss below convolute basal reflections (Figure 8). Reflections above the basal deposits in GPR profile L2 are discontinuous, but they are generally horizontal to subhorizontal in orientation. The upward transition from shallow cut-and-fill reflections to subhorizontal reflections likely represents the vertical accretion of the spit by wave overwash, followed by eolian sand transport and deposition. Net dune accretion in the narrow spit is favored by rising groundwater surface, which follows net sea level rise in the barrier sand systems. No large cut-and-fill reflections (5–10 m height) are observed in the upper 5–10 m of the GPR profile L2.

Line drawings of high-amplitude semi-continuous reflections are constructed for the composite GPR profiles (L1–L11) extending along the full 5-km length of the Nehalem spit (Figure 6). Subhorizontal to horizontal reflections occur throughout the linked profiles, ruling out any evidence of tidal inlet channel breaches during the latest prehistoric or early historic time (Figure 9). Small-scale irregularities, 1–5 m

PETERSON ET AL.

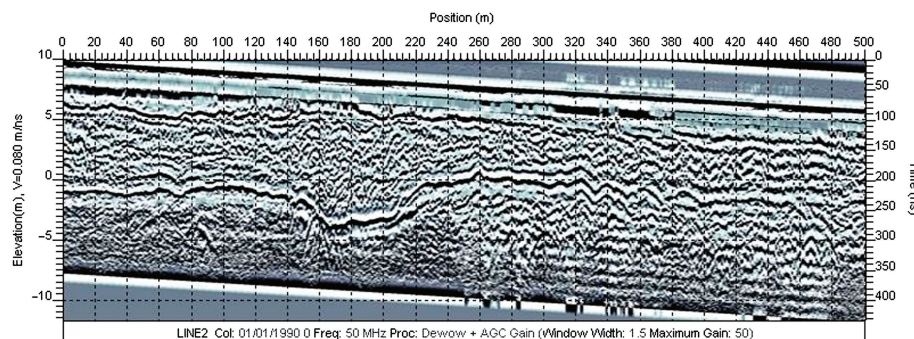


Figure 8. Ground-penetrating radar (GPR) plot from the second north-to-south profile (L2), located near the north end of the Nehalem spit (Figure 7). The profile was collected with a 50-MHz antenna mounted on a trailer system. Topographic control is provided at profile endpoints (~500 m distance intervals).

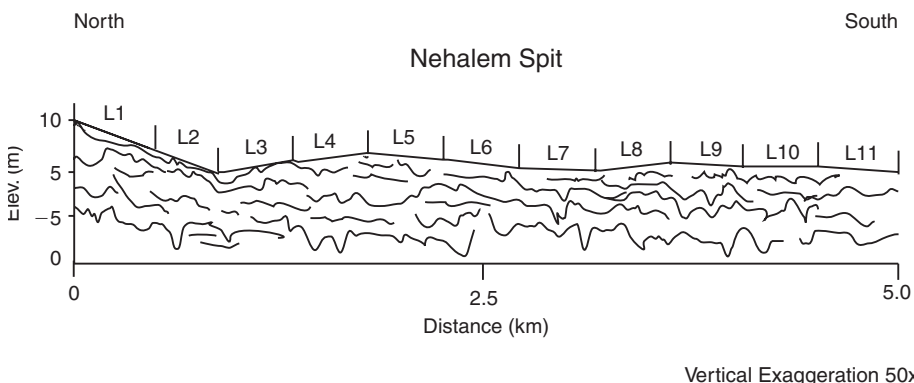


Figure 9. Line diagram of high-amplitude semicontinuous reflections from linked GPR profiles (L1-L11) in the Nehalem spit (Figure 7). No large cut-and-fill features or epsilon strata are imaged in the upper 10 m of the spit deposits.

in depth, are common in the GPR reflections, and likely indicate localized scouring and/or deflation between periods of net vertical accretion.

Across-shore GPR profiling of the Nehalem spit ocean beaches was performed to test for recent changes in shoreline position (Figure 6). These profiles demonstrate a large beach retreat scarp that extends about 100 m landward of the present beach (Figure 10). This latest, or most seaward, scarp in the prograded Nehalem spit corresponds to the last Cascadia rupture and coseismic subsidence event at A.D. 1700 (Table I). The retreat scarp is of catastrophic scale by comparison to erosion from historic winter storm events. However, the backedge of the retreat scarp does not reach the spit interior, which is reported to host wreck timber artifacts. The retreat scarp is entirely buried by the modern foredune. Attempts to hand-probe with sand auger to the retreat scarp were unsuccessful due to either penetration refusal in

GEOARCHAEOLOGY OF THE NEHALEM SPIT

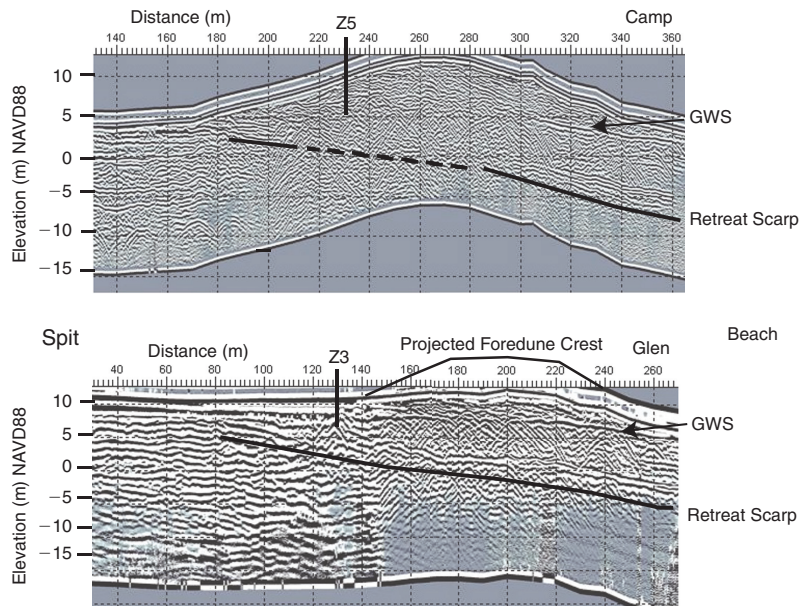


Figure 10. Across-shore GPR profiles from the Nehalem spit (Figure 7), crossing the modern foredune and terminating at the saltwater intrusion interface (beach backshore) at right. Large beach retreat scarps are imaged under the modern foredune. Sand auger probes Z5 and Z2 (Table II) failed to reach the deeply buried retreat scarp due to hole collapse at the groundwater surface (GWS).

large debris, which was not recovered, or hole collapse at the groundwater surface (Table II).

Subsurface Probes

The small-scale stratigraphic development of the shallowest spit deposits (1–3 m depth), are revealed in auger probe, trench, and bayshore cutbank sites (Figure 6, Table II). Very well-sorted dune sand predominates in all of the shallow groundtruth sites. Probe depths were limited by hole collapse in saturated sand deposits at the groundwater surface (GWS), at 1–3 m depth in many sites.

Anomalous large clasts, including pebbles (less than 6.5 cm Di), cobbles (6.5–25.6 cm Di), and small boulders (greater than 25.6 cm Di) are found in 12 subsurface sites from the middle section of the spit, between sites A10 and T20 (Figure 6, Table II). The large clasts occur in one or two distinct layers, which are distinguished by dark sand that contains granule-size lithic fragments (Figure 11). The uppermost large clast layer is correlated between probe sites that cross the interior of the spit's middle section (Figure 12). In one transect (CB13 to T16), the uppermost large clast layer overlies a buried beach cobble berm on the west side of the spit interior at T16.

The large clast layer(s) reflect catastrophic flooding event(s) that crossed the middle section of the Nehalem spit (Figure 12). The large clast layers in the spit interior

PETERSON ET AL.

Table II. Auger probe, cutbank, and trench sites in the Nehalem Bay spit.

Site	UTM-N (m)	UTM-E (m)	Elevation (m) NAVD88	Total Depth (cm)	1st Clast Layer Depth (cm)	2nd Clast Layer Depth (cm)
Z1*	5062302	426886	10	450	450	
Z2*	5062316	426872	12	465	450	
Z3*	5061532	426929	10	525	525	
Z4	5061593	427287	12	225		
A1	5061405	427624	10	185		
A2	5061339	427578	9	115		
A3	5061290	427484	9	190		
A4	5061189	427491	8	150		
Z5*	5061165	426975	10	415		
Z6	5061132	427164	7	235		
A5	5061073	427515	7	80		
A6	5060882	427565	6	120		
A7	5060756	427576	5	130		
A8	5060613	427548	4	140		
A9	5060392	427464	2	195		
A10	5060259	427316	3	205	120–130	
A11	5060139	427256	2	165	80–90	
CB12	5059749	427169	2	105	12–29	
Z7*	5059615	426986	8	360	360	
CB13	5059396	427154	2	205	57–78	150–160
T14	5059389	427110	2	120	23–30	110–120
T15	5059389	427110	3	140	110–130	
T16	5059500	427033	5	95	10–95	
CB17	5059211	427169	2	201	80–100	190–200
CB18	5058633	427176	2	205	50–57	103–160
A19	5058620	427166	3	130	15–30	115–125
T20	5058620	427100	4	265	130–152	190–194
A21	5057693	427204	4	265		
A22	5057022	427100	5	285		

* Auger sites taken near extrapolated backedge of GPR beach retreat scarp. Penetration refusal in clasts, debris, or water table prohibited sample recovery with hand sand auger. Mechanical testing is required.

occur 100–200 m seaward of the reach of the 1964 river flood, as documented by remnant drift logs from the 1964 high water line. The 1964 flood represents a 100–500 year flood in many rivers of the north Oregon coast. No historic cobble or pebble deposits are associated with the 1964 high water line. The presence of large cobbles in discrete strata that cross the spit argue for catastrophic flooding that far exceeds 100–500 yr river flooding in the lower Nehalem Bay. The cobble sheets are interpreted to be of tsunami origin.

A sand sample was taken from a depth of 100 cm in cutbank site CB13 for optically stimulated luminescence (OSL) dating by James Feathers at the University of

GEOARCHAEOLOGY OF THE NEHALEM SPIT



Figure 11. Catastrophic flood deposit (dark lithic-rich sand with cobbles) at 60–70 cm depth exposed in spit deposits (light quartz-rich dune sand) in cutbank of Nehalem spit (site CB13) (Figure 8, Table II). Vertical measuring stick scale is 140 cm in length. An optically stimulated luminescence (OSL) sample was collected just below the cobble layer at 100 cm depth (see Figure 13 for full stratigraphic section).

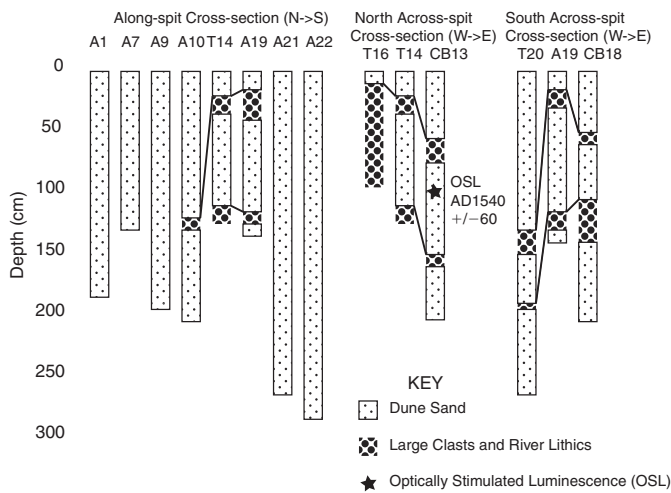


Figure 12. Cross-sections of large clast layers in the middle section of the Nehalem spit. The optically stimulated luminescence (OSL) sample (LAB#UW2182) is from 100 cm depth, located between the upper and lower target tsunami cobble sheets. The reported OSL age A.D. 1540 ± 60 (1-sigma error) correlates the upper cobble sheet to the A.D. 1700 Cascadia great earthquake tsunami. The lower cobble sheet is expected to correlate to either Cascadia events #2 or #3 (Table I) based on the overlying sample age of A.D. 1540 ± 60.

PETERSON ET AL.



Figure 13. Tsunami clasts exposed in a dune deflation hollow in the middle section of the Nehalem spit (site C19 in Figure 8). The largest cobbles shown here reach 10–15 cm in intermediate diameter (D_i). Smaller pebbles are hidden by vegetation. Clasts were lifted free of the surface prior to measurement of intermediate diameters.

Washington (Figures 11, 12). This depth is located between the upper and lower cobble layers. The sample (UW2182) returned a date of A.D. 1540 ± 60 , based on 40 K-feldspar grains. The date is based on single-grain IRSL analysis of K-feldspars, using the protocol of Auclair, Lamothe, and Huot (2003), and fading correction using Huntley and Lamothe (2001). A central age model is used to express the central tendency at ± 1 -sigma analytical error (Galbraith et al., 1999). The age of the sand layer (\sim A.D. 1540) from between the two cobble sheets directly correlates the upper cobble sheet to the A.D. 1700 Cascadia great earthquake and tsunami (Table I).

Several shallow probes were taken at sites near the backedges of large retreat scarps that are buried under the modern foredunes (Figure 6). Penetration refusal occurred in large debris of unknown character in Z1, Z2, and Z3 (Table II). Hole collapse at the GWS prevented probing to the estimated depth of the large beach retreat scarps in Z3 and Z5. Mechanical augering is needed to reach the retreat scarp targets in the Nehalem spit. However, an older retreat scarp anomaly, imaged in GPR line HORS (Figure 6), was likely encountered in T16, where cobbles were packaged in a buried beach berm feature (Figure 12).

Tsunami Cobble Sheet

The shallowest or uppermost tsunami clast layer is traced to surface exposures in deflation hollows, downcut horse trails, and in shoreline cutbanks of the Nehalem spit (Figure 13). The clasts are widely distributed across the Nehalem spit, forming a tsunami cobble sheet, which is locally exposed in the spit deflation plain. The clast abundance, maximum clast size, and mean clast size are presented for 49 cobble sites (Table III).

Table III. Sites containing large clasts exposed at the surface of the Nehalem spit.

Site	UTM-N (m) EPE ± 5 m	UTM-E (m) EPE ± 5 m	Elevation (m) NAVD88	Clast Number in Plot Area	Maximum Clast Size (cm)	Mean Clast Size (cm)	Std. Dev. 1σ
C1	5060162	427150	5	3	34	21	12
C2	5060129	427173	4	6	37	14	4
C3	5060111	427161	2	4	24	17	4.7
C4	5060014	427183	3	21	9.1	3.6	2.4
C5	5059862	427077	5	25	35	4.8	1.9
C6*	5059823	427201	3	7	12.5	7.9	3.3
C7	5059780	427186	2	8	13.2	9.4	1.4
C8	5059768	427095	5	3	10	10	3.5
C9	5059758	427116	4	12	28.0	10.3	6
C10	5059699	427168	2	3	40	15	2.5
C11	5059692	427202	1	25	14	3.6	1.5
C12*	5059628	427073	5	26	15	4.3	2.2
C13	5059610	427160	3	5	24	12	3.8
C14	5059532	427119	3	10	23.3	8.2	3.8
C15	5059530	427178	1	15	26.7	13.1	7.4
C16	5059512	427032	5	10	16.1	6.6	3.5
C17	5059449	427072	4	3	24	12.7	7
C18	5059419	427069	4	5	16	10	3.2
C19*	5059408	427116	3	14	16	7.1	4.1
C20	5059398	427158	1	19	28.5	6.2	3.2
C21*	5059336	427112	3	20	18	3.8	2.4
C22	5059269	427109	5	23	14	5.5	2.6
C23	5059257	427050	4	10	18	10	3.7
C24*	5059193	427133	3	22	19	4.7	2.6
C25	5059055	427123	3	17	21	9.4	4.4
C26	5059052	427063	4	14	16	8	3.5
CP#1	5059046	427121	4	1 sherd	6	—	—
C27*	5059039	427177	2	12	22	8	5
C28	5058959	427063	4	11	14.2	7.4	3.1
C29*	5058920	427192	1	20	14	6.2	3.5
C30	5058703	427195	2	23	14.5	4.4	2.1
C31	5058632	427100	2	21	14	7.3	2.3
C32*	5058590	427071	4	25	4	2.5	0.9
C33	5058539	427312	1	25	10.5	3.2	7.5
C34	5058522	427135	3	7	4.5	6.3	2.5
C35	5058498	427137	3	7	12.3	8.2	3.5
C36	5058443	427160	3	11	14.4	8.3	4.1
C37	5058384	427150	3	5	14.4	11	1.7
C38	5058302	427207	3	5	13	4.5	3.6
C39*	5058297	427129	3	3	11.1	8.2	4
C40	5058203	427231	3	1	11	11	—
C41	5058057	427313	2	1	4	4	—
C42	5057976	427059	4	2	5	4	0.7
C43	5057971	427301	2	5	14	7.4	2.6
C44†	5057920	427233	3	8	12.5	9.3	1.9
C45	5057886	427311	3	5	14	5.9	1.7
C46†	5057765	427200	3	7	2.7	2.3	0.8
C47	5057680	427263	2	2	2.5	2.2	0.3
C48†	5057632	427238	3	8	6.5	4.2	1.7
C49†	5057609	427237	2	5	2.5	2.3	0.4

Note: Plot area size is shown as follows: 1.0 m² (default), ~0.5 m² (†), and ~10 m² (*).

Mean and standard deviation (SD in cm) are based on the total clast number counted for the plot area.

CP#1 is the Chinese porcelain sherd exposed in a trail that crosses the exposed tsunami cobble layer in the central part of the Nehalem spit (see Figures 3, 8, and 16).

PETERSON ET AL.

Table IV. Lithologies of A.D. 1700 tsunami cobbles and of end member cobble sources from the beach and the Nehalem River.

Lithology	Tsunami C9, C19	Beach	River Main	River NF
Gabbro-diabase, Columbia River Basalt (CRB) Fm	3	27	2	3
Aphyric basalt or basaltic-andesite, undifferentiated Fm	4	3	7	5
Porphyritic basaltic-andesite, or andesite, Tillamook Volcanics	6	0	8	5
Aphyric basaltic-andesite, or andesite, Tillamook Volcanics	6	0	6	3
Porphyritic pyroxene or plagioclase basalt, Tillamook Volcanics	4	0	5	3
Vesicular basalt, basaltic-andesite, andesite, or dacite, Tillamook Volcanics	3	—	2	1
Baked pebbly sandstone, or coarse sandstone, Astoria Fm	1	0	0	0
Baked burrowed mudstone-siltstone, Smugglers Cove Fm	2	0	0	6
Baked tuffaceous siltstone-mudstone, Oswald West Fm or Kesey Fm	1	0	0	4
Total	30	30	30	30

Note: Cobbles from the Main and North Forks (NF) of the Nehalem River were each collected at bridge sites about 15 km upriver of their mutual confluence at UTM 5063530n, 439950e, and UTM 507358-n, 440140e, respectively. Cobbles from the Manzanita beach cobble berm (Beach) were collected about 1.5 km southeast of the Neahkahnie headland. Cobble lithologies were indentified from fresh fracture faces examined under hand lens. Cobble lithologies are tied to bedrock units in the Neahkahnie headland and in the Nehalem River drainages following Niem and Niem (1985) and Wells et al. (1994).

The tsunami clasts mantle the full width and length of the middle section of the Nehalem spit, extending over a surface area of 2.25 km² (Figure 7). The maximum clast size ranges from 3 to 40 cm in intermediate diameter (Table III). Clast abundance and size generally decrease from north to south along the spit. A trend surface analysis confirms a fining of clast size from north to south at greater than 95 percent confidence interval. No significant across-spit trends of clast abundance or size are apparent in the 49 sites analyzed, possibly due to the narrowness of the spit.

The presence of the A.D. 1700 tsunami cobble sheet throughout much of the Nehalem spit confirms the integrity and stability of the spit since early historic times in the area. The second tsunami cobble sheet (Figure 12) must correlate to an older Cascadia tsunami of about 1000 yrs in age (Table I), indicating stability of the middle spit section back to that time period.

The trends of decreasing clast size with distance south of the Nehalem channel bend at Fishery Point suggest a cobble origin from the Nehalem channel. To establish the origin of the tsunami cobbles, their representative lithologies are compared to end member samples from the Nehalem River and from a beach cobble berm at the base of the Neahkahnie headland (Table IV). The Neahkahnie Mountain headland is formed

GEOARCHAEOLOGY OF THE NEHALEM SPIT

from the gabbro-diorite Columbia River Basalt (CRB) Grand Ronde flow (Niem & Niem, 1985). The beach cobbles (90% gabbro-diorite CRB) directly reflect this source lithology. The Nehalem drainage contains a wide variety of volcanic and sedimentary formations with distinctive lithologies (Niem & Niem, 1985; Wells et al., 1994). The drainage of the Nehalem Main Fork is much larger than the Nehalem North Fork, but the North Fork contains some very distinctive sill-baked sedimentary rocks. The tsunami cobbles from sites C9 and C19 reflect the mixed lithologies of the Nehalem River source(s), and not the nearly uniform lithology of the beach cobbles from the Neahkahnie Mountain volcanic sill. The tsunami cobbles on the Nehalem spit are derived from tsunami return flow(s) directed down the Nehalem Channel and around Fishery Point. This is the first reported evidence of tsunami backwash flow inundation and associated large clast deposition in the Cascadia margin.

Recently, a porcelain sherd associated with the wreck was found on the Nehalem spit (Figure 2), exposed on the surface of the tsunami cobble layer (G. McDaniel, Oregon State Parks, personal communication, 2010) (Figure 7). The sherd was exposed in a horse trail (Table III) that crosses the tsunami cobble layer. Although it could not be determined if the sherd was deposited with the cobbles by the tsunami or had been dropped on the cobble surface at a later date, the location away from any known Indian sites on the spit combined with the relatively large size of the sherd suggests that the cobble layer may contain *in situ* sherds, deposited by the reversing tsunami surges but originating from wrecked cargo scattered on the beach or just offshore. The fragment is 6 by 3.5 cm in size, and it contains a blue-on-white floral scroll motif of either a tiger lily or a modified chrysanthemum.

DISCUSSION

A wrecked Manila galleon would have littered the Nehalem area shorelines with abundant cargo and ship structural debris (Konstam, 2004) and beeswax, which was a cargo that only the Spanish shipped (Schurz, 1939; Marshall, 1984; Williams, 2007; Figure 1). Pioneers routinely collected these artifacts from the Nehalem spit beaches in the mid to late 19th century (Giesecke, 2001; Williams, 2007). Finds of either teak wood or beeswax blocks from the Nehalem ocean beaches became rare by the mid-1900s (Giesecke, 2007; Williams, 2007).

We propose the following sequence of events to have distributed, and then buried, the Beeswax wreck debris on the Nehalem spit. A Spanish galleon, possibly the *Santo Christo de Burgos*, lost in A.D. 1693, wrecked offshore of the Nehalem spit area in the late 1600s (Lally, 2008). The wreck debris was distributed along the spit and/or the Neahkahnie headland area by seasonally reversing currents for several years or decades. The A.D. 1700 Cascadia earthquake produced a moderate-sized tsunami runoff in the Nehalem area (Schlichting, 2000) that swept wreck debris across the Nehalem spit and into Nehalem Bay. Tsunami backwash from Nehalem Bay was directed down the Nehalem channel and over the low-lying sections of the middle spit (Figure 14). Shallow reversing surges could account for the chaotic deposition of mixed beach sand, coarse river sand, and river cobbles in thin tsunami layers

PETERSON ET AL.

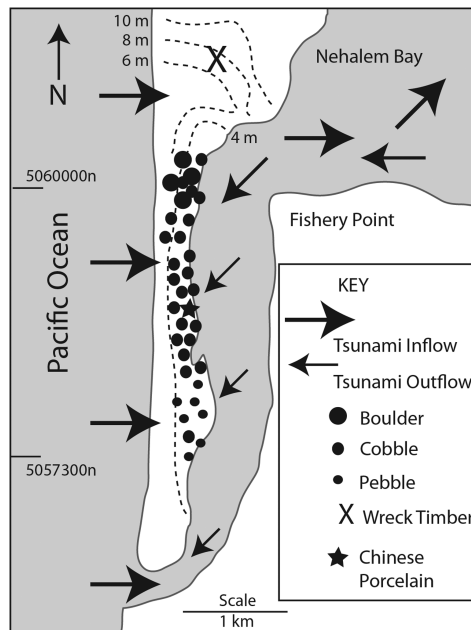


Figure 14. Map of tsunami maximum clast size (boulders, cobbles, pebbles in black circles) from representative surface exposure sites in the Nehalem spit. Tsunami inflow and outflow (arrows), reported wreck teak timbers (X), and recently discovered Chinese porcelain (black star) are shown relative to modern elevations (dotted lines in m NAVD88) in the spit deflation plain. Modern foredune elevations at the ocean beach are not shown.

across the spit interior. Shipwreck porcelain and earthenware sherds from shipwreck debris on the spit beaches were remobilized and deposited over the middle spit by the reversing tsunami surges. Wreck debris was better retained in the north spit in tsunami inflow strandlines (~6–8 m elevation) that exceeded the heights of the tsunami return flows (~4–6 m elevation) over the middle spit.

Wreck debris deposited on the Nehalem Bay tidal flats, by tsunami inundation over the Nehalem spit, has been buried by interseismic sedimentation (40–80 cm) (Figure 4) that followed the coseismic coastal subsidence from the A.D. 1700 rupture. The regional coseismic subsidence, ~1.5 m in Nehalem Bay (Grant, 1994), led to catastrophic beach retreat (Figure 10). Remaining Beeswax wreck debris on the ocean beach was carried landward against the retreating beach face by winter surf. The wreck debris is reported to have remained exposed until settlers reached the coast in the early 1800s (Geisecke, 2007; Marshall, 1984). Following interseismic rebound and uplift, the beach began to recover, eventually burying wood and wax artifacts in strandlines under beach progradation and foredune accretion by the early 1900s.

The interseismic accretion of the Nehalem spit is measured by horizontal displacement of the 0 m datum intercept between the coseismic beach retreat scarp and

GEOARCHAEOLOGY OF THE NEHALEM SPIT

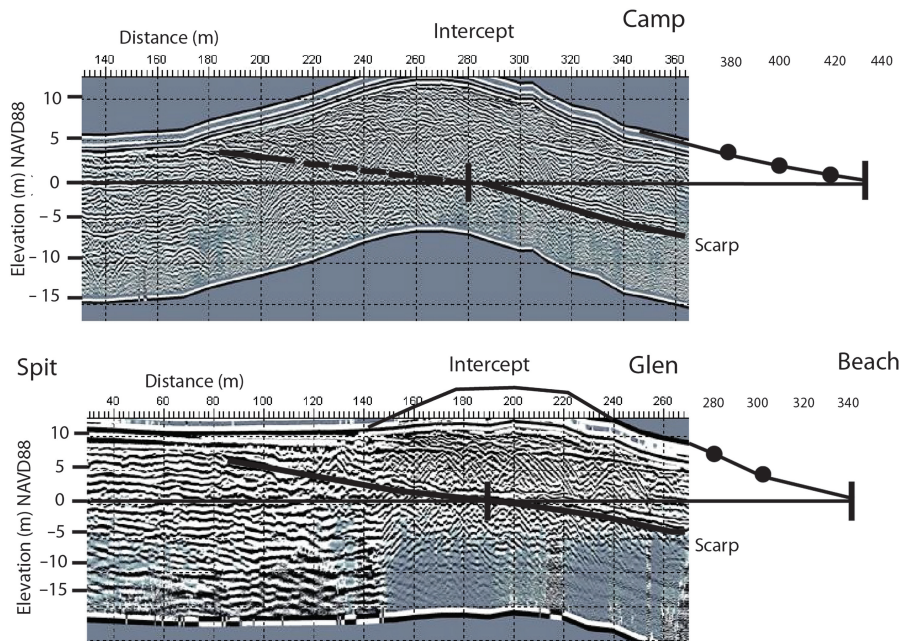


Figure 15. Beach recovery and net accretion to present time since catastrophic retreat at A.D. 1700. Topographic surveying was carried seaward of the saltwater limitation of GPR recording, as shown by solid circles. Profile extension to -1 m MTL is based on gradients measured in the Nehalem spit during previous beach surveys (Doyle, 1996).

the modern beach face. The beach progradational recovery is measured at two GPR profiles, Camp and Glen (Figure 15). The measured beach recovery is ~ 150 m in across-shore distance. Assuming no net gain or loss of beach sand from the Nehalem nearshore during the last 300 years, the measured beach recovery possibly reflects the coseismic retreat distance. Catastrophic retreat of ~ 150 m, following 1.5 m of coastal subsidence, is within tolerances of predicted beach retreat using the modified Brunn relation for the Nehalem spit setting (Doyle, 1996).

Northward migration or fluctuation of the Nehalem tidal inlet prior to jetty stabilization in the early 1900s probably accounts for the sightings of wreck debris at the south end of the spit at the turn of the century (Williams, 2008). The relatively recent finds of teak wood at the north end of the spit likely reflects the lack of net sand accretion at the south side of the Neahkahnie headland. Episodic erosion exposes beach boulder berms near Manzanita, possibly releasing trapped wreck debris.

Dune sand migration over the spit occurred until the mid 1900s (Cooper, 1958), when non-native dune grass stabilized the foredune, and deflation locally exposed the spit interior. Sand dunes ramped up against the south side of the Manzanita dune sheet (see Figure 16 below), possibly burying the A.D. 1700 tsunami strand line.

PETERSON ET AL.

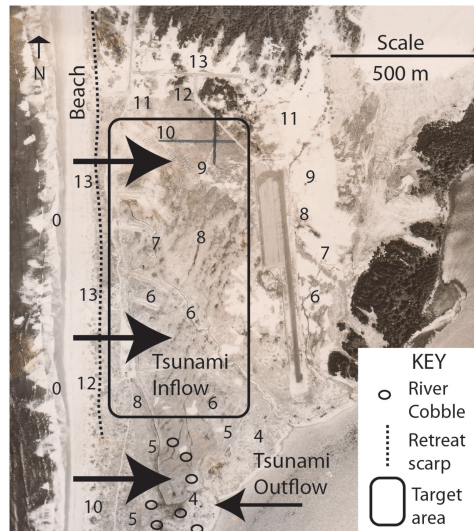


Figure 16. Historic (1960) air photo of the north end of the Nehalem spit, showing (1) early foredune and deflation plain morphology, (2) modern spot elevations, (3) mapped A.D. 1700 beach retreat scarp (dotted line), (4) A.D. 1700 tsunami outflow cobbles (open circles), and most likely preservation of buoyant artifacts including wood and wax (box) in areas of tsunami inflow strandlines in the spit interior.

However, deflation dominated in the middle spit section, thereby locally exposing the A.D. 1700 tsunami cobble sheet. At least one pioneer traced a “freshet silt layer” (i.e., the tsunami debris layer) under the dune sand to find beeswax candles and other shipwreck artifacts in the spit interior (Hult, 1968; Oregon Native Son, 1900).

Episodic erosion of the Nehalem spit bayshore locally entrenches the bayside cutbanks, which release unworked earthenware and porcelain sherds from the A.D. 1700 tsunami sand and cobble layer. Channel bank erosion at Cronin Point is also releasing worked porcelain sherds and debitage, which are transported north to bay flats by tidal flood and wind-wave currents (Figure 1). The flaked porcelain found along the bay shoreline south of Fishery Point could be related to the use of this shoreline as a travel route in late prehistoric and early historic time.

Wreck Debris Target Areas

The northward limit of tsunami river cobbles in the Nehalem spit probably marks the northward extent of tsunami outflow over the spit (Figure 14). The lower outflow heights, relative to higher inflow heights, should preserve the tsunami inundation strandline(s) and any accompanying wreck woody debris. We target an area that should have the highest probability of preserving wreck timber and beeswax associated with the A.D. 1700 tsunami inflow strandline(s). The target area is based on the following criteria: (1) predicted tsunami runup (A.D. 1700 event) not exceeding

GEOARCHAEOLOGY OF THE NEHALEM SPIT

8 m (Peterson et al., 2008), (2) modern spit interior heights (5–10 m elevation), (3) historic accounts of wreck wood debris (Giesecke, 2007), (4) dune cover of 1–3 m thickness (Table II), and (5) the limit of outflow cobble deposition (Figure 16).

Foredune accretion has likely buried debris at the back edge of beach retreat scarps below the reach of hand probing (Figure 16). However, deflation behind the foredune could put the wreck debris within reach of shallow probing or trenching. The more deeply buried retreat scarp, and any associated post–A.D. 1700 beach strandline debris, located under the foredune will require mechanical drilling for artifact recovery and wreck debris verification.

The wreck's heavy cargo is likely located offshore of the Nehalem spit or Neahkahnie headland. An offshore wreck site will require offshore surveying for exposed debris and/or magnetic artifacts. The return of offshore sand to the beaches, during the last 100 years of interseismic recovery (Figure 15), could re-expose offshore Beeswax wreck debris. Optimal exposure would occur if the galleon ran aground within a conservative depth of closure (less than 20 m water depth) in the Nehalem area (Doyle, 1996).

Impact of A.D. 1700 Tsunami and Coastal Subsidence on Nehalem Archaeological Sites

Nehalem–Tillamook flooding myths were recounted in 1934 by Clara Pearson (Jacobs & Jacobs, 1959), who was reported to be one of the last fluent speakers of the Nehalem language on the Oregon coast (Woodward, 1990). Whether or not the recorded myths refer to the A.D. 1700 Cascadia tsunami, there is physical evidence of archaeological site impact(s) from the event in Nehalem Bay. Abrupt subsidence burial of a Native American occupation site (35T156) is reported from an intertidal reach of the North Fork of the Nehalem River (Figure 2) (Minor & Grant, 1996). The timing of the radiocarbon-dated occupation (660 ± 60 yr B.P. hearth charcoal date) slightly predates the age of the buried forest floor (430 ± 60 yr B.P.) and the age of a possible tsunami sand (370 ± 60 yr B.P.) (Minor & Grant, 1996). However, the estimated submergence (1.5 m) would have made wetland sites in Nehalem Bay uninhabitable for decades following the coseismic subsidence.

Additional evidence of impact from the A.D. 1700 event is found at Cronin Point 35TI4 (Figure 1), where a horizon with fire-cracked rock is buried by woody debris and silt. A woven mat in the top of the debris layer is dated at 380 ± 60 yr B.P. (Woodward, 1986b). The wood and silt layers are interpreted to represent tsunami debris layer from the A.D. 1700 event (Woodward, 1990). In this study we confirm the inundation and burial of the Cronin Point site by the A.D. 1700 tsunami, which inundated the full extent of the northern Nehalem Bay (Figure 4). Though this event was temporarily catastrophic to some low-lying shorelines, the Native Americans did not permanently abandon their occupation sites in Nehalem Bay (Losey, 2002).

Catastrophic tsunami inundation and/or post-subsidence burial of Native American occupation sites, at about A.D. 1700, are also reported from Willapa Bay and the Copalis River mouth area in southwest Washington (Figure 1) (Cole et al., 1996).

PETERSON ET AL.

The study presented here and its relation to the Beeswax wreck debris is the first report of the A.D. 1700 tsunami and coseismic subsidence impacting an early European archaeological site in the Cascadia margin.

CONCLUSIONS

This study of the geomorphology, littoral processes, and coseismic impacts on the Nehalem spit argue for a Beeswax shipwreck date that precedes the last Cascadia earthquake and tsunami at ~A.D. 1700. Shipwreck teak wood, beeswax, and Chinese porcelain sherds were carried over the spit by tsunami inflow. Wreck debris is likely preserved on the higher north spit section, located above the reach of tsunami outflow. A widespread river-cobble sheet represents the course of tsunami outflow over the lower mid-spit section. Coseismic subsidence resulted in catastrophic beach retreat, which remobilized post-tsunami beach debris to more landward beach strandlines. However, interseismic beach recovery and recent foredune accretion have buried the catastrophic retreat strandlines and associated wreck debris during the last 150 years. The concurrent onshore movement of nearshore sand could expose some offshore heavy wreck debris if the ship wrecked in shallow water. These results provide intriguing evidence of an important early shipwreck site that was impacted by the A.D. 1700 tsunami and post-subsidence beach retreat in the central Cascadia margin. Perhaps the greatest significance of the Beeswax wreck is that it represents the earliest archaeological evidence of contact between Euroamericans and Native Americans on the northern Oregon coast.

Rick Rogers served as co-leader of the Beeswax Wreck Team. Eb Giesecke pointed out reported sites of wreck artifacts from the interior of the Nehalem spit. Alan Niem performed the cobble lithology identifications and, together with Wendy Niem, provided the cobble lithology correlations to mapped bedrock formations in the Nehalem River drainages. Dave Wellman performed Total Station-Opus GPS surveying. Bill Spurlock provided details about galleon construction and characteristics of wreckage debris. Paul See provided descriptions of wreck timber being harvested from the Manzanita shorelines during the early 1900s. In 2007, Timothy Blazina, Darrick Boschman, Scott Braunsten, Mathew Brown, Ezzell Brandon, Adam Cambell, Annie Donehey, Erin Dunbar, Aspen Gillam, Thomas Schepker, Joshua Theule, and Stephen Wilson assisted with preliminary GPR profiling, total station surveying, and sand auger probing. In 2009, Kate Mickelson, Kendra Williams, Beth Paulson, Kristin McGlothen, Stacy Smith, and Hollie Heesacker performed auger and trench probing and tsunami clast size measurement. Galen Peterson assisted with OSL sampling in bayside cutbank exposures of the Nehalem spit. Russ Mathews provided GPR maintenance fees support. Lewis Scott and the Naga Research Group provided support for radiocarbon dating. The Oregon State Park at Nehalem Bay, Oregon, provided access and logistical support. Gary McDaniel assisted with Chinese porcelain artifact collection on the Nehalem spit in 2010. We thank Rick Minor, Jon Erlandson, and an anonymous reviewer for helpful comments that improved this manuscript.

REFERENCES

- Atwater, B.F., Tuttle, M.P., Schweig, E.S., Rubin, C.M., Yamaguchi, D.K., & Hemphill-Haley, E. (2004). Earthquake recurrence, inferred from paleoseismology. In A.R. Gillespie, S.C. Porter, & B.F. Atwater (Eds.), *The Quaternary period in the United States* (pp. 331–350). Amsterdam: Elsevier.
- Auclair, M., Lamothe, M., & Huot, S. (2003). Measurement of anomalous fading for feldspar IRSL using SAR. *Radiation Measurements*, 37, 487–492.

GEOARCHAEOLOGY OF THE NEHALEM SPIT

- Barnett, E.T. (1997). Potential for coastal flooding due to coseismic subsidence in the central Cascadia margin. Unpublished master's thesis, Portland State University, Portland, Oregon.
- Beals, H.K., & Steele, H. (1981). Chinese porcelains from site 35-TI-1, Netarts sand spit, Tillamook County, Oregon. *University of Oregon Anthropological Papers No. 23*. Portland: University of Oregon.
- Cole, S.C., Atwater, B.F., McCutcheon, P.T., & Stein, J.K. (1996). Earthquake-induced burial of archaeological sites along the southern Washington coast about 1700 AD. *Geoarchaeology*, 11, 165–177.
- Cooper, W.S. (1958). Coastal sand dunes of Oregon and Washington. *Geological Society of America Memoir 72*. New York: Geological Society of America.
- Darrienzo, M.E., & Peterson, C.D. (1995). Magnitude and frequency of subduction-zone earthquakes along the northern Oregon coast in the past 3,000 years. *Oregon Geology*, 57, 3–12.
- Darrienzo, M.E., Peterson, C.D., & Clough, C. (1994). Stratigraphic evidence for great subduction zone earthquakes at four estuaries in northern Oregon. *Journal of Coastal Research*, 10, 850–876.
- Doyle, D.L. (1996). Beach response to subsidence following a Cascadia subduction zone earthquake along the Washington-Oregon coast. Unpublished master's thesis, Portland State University, Portland, Oregon.
- Erlandson, J., Losey, R., & Peterson, N. (2001). Early maritime contact on the northern Oregon coast: Some notes on the 17th century Nehalem Beeswax ship. In J. Younker, M. Tveskov, & D. Lewis (Eds.), *Telling out stories: Proceedings of the fourth annual Coquille Cultural Preservation Conference* (pp 45–53). North Bend, OR: Coquille Indian Tribe.
- Galbraith, R.F., Roberts, R.G., Laslett, G.M., Yoshida, H., & Olley, J.M. (1999). Optical dating of single and multiple grains of quartz from Jinmium rock shelter, northern Australia, Part I: Experimental design and statistical models. *Archaeometry*, 41, 339–364.
- Giesecke, E.W. (2007). *Beeswax, teak, and castaways: Searching for Oregon's lost protohistoric Asian ship*. Manzanita, OR: Nehalem Valley Historical Society.
- Grant, W.C. (1994). Paleoseismic evidence for late Holocene episodic subsidence on the northern Oregon coast. Unpublished master's project, University of Washington.
- Heaton, T.H., & Kanamori, H. (1984). Seismic potential associated with subduction in the northwestern United States. *Bulletin of the Seismological Society of America*, 74, 933–941.
- Hult, R.E. (1968). *Lost mines and treasures of the Pacific Northwest*. Portland, OR: Binford & Mort.
- Huntley, D.J., & Lamothe, M. (2001). Ubiquity of anomalous fading in K-feldspars and the measurements and correction for it in optical dating. *Canadian Journal of Earth Science*, 38, 1093–1106.
- Jacobs, E.D., & Jacobs, M. (1959). *Nehalem Bay tales*. Monographs, Studies in Anthropology. Eugene, OR: University of Oregon.
- Jol, H.M., & Bristow, C.S. (2003). GPR in sediments: Advice on data collection, basic processing and interpretation, a good practice guide. In C.S. Bristow & H.M. Jol (Eds.), *Ground penetrating radar in sediments* (pp. 9–27). Special Publication No. 211. London: Geological Society of London.
- Jol, H.M., Smith, D.G., & Meyers, R.A. (1996). Digital ground penetrating radar (GPR): An improved and very effective geophysical tool for studying modern coastal barriers (examples for the Atlantic, Gulf and Pacific coasts, U.S.A.). *Journal of Coastal Research*, 12, 960–968.
- Komar, P.D. (1992). Ocean processes and hazards along the Oregon coast. *Oregon Geology*, 54, 65–76.
- Komar, P., Lanfredi, N., Baba, M., Dean, R., Dyrer, K., Healy, T., Terwindt, J., & Thom, B. (1991). The response of beaches to sea-level change: A review of predictive models. *Journal of Coastal Research*, 7, 895–921.
- Konstam, A. (2004). *Spanish galleon 1530–1690*. Oxford: Osprey Publishing.
- Lally, J. (2008). Analysis of the Chinese porcelain associated with the “Beeswax wreck,” Nehalem, Oregon. Unpublished master's thesis, Department of Anthropology, Central Washington University, Ellensburg, Washington.
- Lévesque, R. (2002). *History of Micronesia*. Gatineau, Québec: Lévesque Publications.
- Losey, R.J. (2002). *Communities and catastrophe: Tillamook response to the AD 1700 earthquake and tsunami, Northern Oregon coast*. Unpublished PhD thesis, University of Oregon, Eugene, Oregon.
- Marshall, D. (1984). *Oregon shipwrecks*. Portland, OR: Binford & Mort.
- Meyers, R.A., Smith, D.G., Jol, H.M., & Peterson, C.D. (1996). Evidence for eight great earthquake-subsidence events detected with ground-penetrating radar, Willapa barrier, Washington. *Geology*, 24, 99–102.
- Minor, R., & Grant, W.C. (1996). Earthquake-induced subsidence and burial of the late Holocene archaeological sites, Northern Oregon Coast. *American Antiquity*, 61, 772–781.

PETERSON ET AL.

- Niem, A.R., & Niem, W.A. (1985). Geologic map of the Astoria Basin, Clatsop and northernmost Tillamook Counties, northwestern Oregon. Oil and Gas Investigation, map OGI-14, State of Oregon Department of Geology and Mineral Industries.
- Oregon Native Son. (1900). North Pacific prehistoric wrecks. *Oregon Native Son*, 2, 223.
- Peterson, C.D., & Darienzo, M.E. (1997). Discrimination of flood, storm and tectonic subsidence events in coastal marsh records of Alsea Bay, central Cascadia margin, USA. In A.M. Rogers, T.J. Walsh, W.J. Kockelman, & G.R. Priest (Eds.), *Assessing and reducing earthquake hazards in the Pacific Northwest, Part 1* (pp. 115–146). USGS Professional Paper 1560.
- Peterson, C.D., Cruikshank, K.M., Jol, H.M., & Schlichting, R.B. (2008). Minimum runup heights of tsunamis from evidence of sand ridge overtopping at Cannon Beach, Oregon, central Cascadia margin, USA. *Journal of Sedimentary Research*, 78, 390–409.
- Peterson, C.D., Doyle, D.L., & Barnett, E.T. (2000). Coastal flooding and beach retreat from coseismic subsidence in the central Cascadia margin, USA. *Environmental and Engineering Geology*, 6, 255–269.
- Peterson, C.D., Jol, H.M., Vanderburgh, S., Phipps, J.B., Percy, D., & Gelfenbaum, G. (2010). Dating of late-Holocene shoreline positions by regional correlation of coseismic retreat events in the Columbia River littoral cell, *Marine Geology*. DOI:10.1016/j.margeo.2010.02.003.
- Peterson, C.D., Stock, E., Hart, R., Percy, D., Hostetler, S.W., & Knott, J.R. (2009). Holocene coastal dune fields used as indicators of net littoral transport: West Coast, USA. *Geomorphology*, 116, 115–134. DOI:10.1016/j.geomorph.2009.10.013.
- Pitcock, H.L., Gilbert, W.E., Huyer, A., & Smith, R.L. (1982). Observations of sea level, wind and atmospheric pressure at Newport, Oregon, 1967–1980. Data Report Reference 82-12. Corvallis, OR: Oregon State University, School of Oceanography.
- Satake, K., Shimazaki, K., Tsuji, Y., & Ueda, K. (1996). Time and size of giant earthquake in Cascadia inferred from Japanese tsunami records of January 1700. *Nature*, 378, 246–249.
- Scheans, D., & Stenger, A. (1990). Letter report: 35-TI-1A and related porcelains. Ms. on file, Oregon State Historic Preservation Office, Salem.
- Schlichting, R.B. (2000). Establishing the inundation distance and overtopping height of paleotsunami from late-Holocene geologic records at open-coastal wetland sites, central Cascadia margin. Unpublished master's thesis, Portland State University, Portland, Oregon.
- Schlichting, R.B., & Peterson, C.D. (2006). Mapped overland distance of paleotsunami high-velocity inundation in back-barrier wetlands of the central Cascadia margin, USA. *Journal of Geology*, 114, 577–592.
- Schurz, W.L. (1939). *The Manila galleon*. New York: E.P. Dutton and Co., Inc. (1959 paperback edition).
- U.S. Coast Survey. (1875). Entrance to Nehalem River, ORE. NE-1-1:1 Map.
- Wells, R.E., Snaveley, P.D., Jr., MacLeod, N.S., Kelly, M.M., & Parker, M.J. (1994). Geologic map of the Tillamook Highlands, Northwest Oregon Coast Range (Tillamook, Nehalem, Enright, Timber, Fairdale, and Blaine 15 minute quadrangles).
- Williams, S. (2007). A research design to conduct archaeological investigations at the site of the “Beeswax wreck” of Nehalem Bay, Tillamook County, Oregon. Ms. on file at Oregon State Parks and Oregon State Historic Preservation Office, Salem.
- Williams, S. (2008). Report on the 2007 fieldwork of the Beeswax Wreck Project, Nehalem Bay, Tillamook County, Oregon. Ms. on file at Oregon State Parks and Oregon State Historic Preservation Office, Salem.
- Woodward, J.A. (1986a). Prehistoric shipwrecks on the Oregon coast? Archaeological evidence. Unpublished report on file at Oregon State Historic Preservation Office, Salem.
- Woodward, J.A. (1986b). Prehistoric shipwrecks on the Oregon coast? Archaeologic evidence. In K. Ames (Ed.), *Oregon Archaeologists Association Proceedings, Third Annual Symposium*, Portland, Oregon.
- Woodward, J.A. (1990). Paleoseismicity and the archaeological record: Areas of investigation on the northern Oregon coast. *Oregon Geology*, 52, 57–65.
- Woxell, L.K. (1998). Prehistoric beach accretion rates and long-term response to sediment depletion in the Columbia River littoral cell. Unpublished master's thesis, Portland State University, Portland, Oregon.

Received 12 July 2010

Accepted for publication 2 December 2010

Scientific editing by Jamie Woodward